scientific reports

Check for updates

OPEN

UV light promoted dihydrolipoic acid and its alanine derivative directed rapid synthesis of stable gold nanoparticles and their catalytic activity

Nimet Temur[1], Seyma Dadi[2], Mustafa Nisari[3], Neslihan Ucuncuoglu[4], Ilker Avan[5] & Ismail Ocsoy[1]✉

In general, colloidal gold nanoparticles (AuNPs) have been synthesized in heated or boiling water containing $HAuCl_4$ precursor with sodium citrate as reducing stabilizing reagent. Although temperature plays a driving for synthesis of AuNPs, elevated temperature in thermal reduction method causes aggregation of the AuNPs. The preferential, rapid and strong binding of dihydro-lipoic acid and its derivatives on surface of AuNPs via thiol – Au chemistry promote the production of very stable AuNPs. In this study, we have developed citric acid (CA), dihydrolipoic acid (DHLA) and DHLA-Alanine (DHLA-Ala) directed rapid synthesis of ultra-stable AuNPs, DHLA@AuNPs and DHLA-Ala@AuNPs, under the UV (311 nm) irradiation at room temperature (RT: 25 °C) in around 10 min (min). CA is used as a potential reducing agent to expedite both reduction of Au^{3+} ion and AuNP formation, DHLA and DHLA-Ala act as stabilizing agents by replacing CA molecules on surface of AuNPs in order to produce quite stable AuNP. It is worthy to mention that reduction of Au^{3+} ion, formation and surface stabilization of AuNPs are consequently occurred in one step. We also investigated how experimental parameters including reaction time and temperature, pH of reaction solution, affect formation of the AuNPs. The effects of salt concentration and storage temperature were studied to show stability of the AuNPs. The synthesized DHLA@AuNPs and DHLA-Alanine@AuNPs were characterized via UV-Vis spectrophotometer (UV-Vis), scanning transmission electron microscope (STEM), dynamic light scattering (DLS) and Zeta potential (ZT) devices. The reduction of 4-nitrophenol (4-NP) to 4-aminophenol (4-AP) was efficiently catalyzed by the AuNPs in the presence of sodium borohydride in aqueous solution.

Keywords Dihydrolipoic acid, Photo-reduction, Ultra-stable Gold Nanoparticle, Catalytic activity

Gold Nanoparticles (AuNP) have been actively used in a wide variety of bioanalytical and biomedical application owing to their easy synthesis with various sizes and shapes, unique and tunable surface plasmon resonance, simple surface engineering and biocompatibility[1–4]. In terms of medical applications, AuNPs have been commonly utilized as promising nano-tools in major medical domains such as imaging or therapeutic and diagnostic applications. In the medical imaging field, AuNPs with the efficient interaction and absorption of corresponding light irradiation are utilized as X-ray, surface enhanced Raman spectroscopy, photoacoustic and optical imaging agents[5–7]. AuNPs are increasingly being explored as promising vehicles for therapeutic applications such as targeted cargo delivery and photothermal therapies (PTT) due to their unique physicochemical properties, tunable surface chemistry and their easy bio-conjugation[8–13]. Since AuNPs are easily conjugated with targeting ligands (DNA aptamers, antibodies and etc.,) and have unique optical features including surface plasmon resonance, they also offer potential use in diagnostics to sense and detect the target molecules[14–20].

[1]Department of Analytical Chemistry, Faculty of Pharmacy, Erciyes University, Kayseri 38039, Turkey. [2]Department of Nanotechnology Engineering, Abdullah Gül University, Kayseri 38080, Turkey. [3]Department of Medical Biochemistry, Faculty of Dentistry, University of Nuh Naci Yazgan, Kayseri 38090, Turkey. [4]Department of Physiology, Faculty of Medicine, Istanbul Medeniyet University, Istanbul 34700, Turkey. [5]Department of Chemistry, Faculty of Science, Eskişehir Technical University, Eskişehir 26470, Turkey. ✉email: ismailocsoy@erciyes.edu.tr

The diverse range of biomedical applications of AuNPs has been marked by the development of a variety of synthesis methods over the years to produce colloidal, uniform, mono-dispersed, stable and biocompatible AuNPs in aqueous media. The AuNPs were synthesized for the first time by the "Turkevich method"[21] which involves using trisodium citrate dihydrate under thermal reduction. The carboxylate groups of citrates bind to surface of AuNPs to prevent their aggregation[22,23], instability of AuNPs in salt solution owing to desorption of the ligand is the major drawback of citrate-based methods. Although researchers reported biomolecules which can direct AuNPs synthesis at room temperature (25 °C), morphology control and positioning of AuNP are considered as remaining issues to be solved[24–26]. The photo-reduction method has been developed as a more noninvasive approach which offers more control over the size, shape, and properties of the synthesized AuNPs by adjusting parameters such as light intensity, duration of light exposure, and concentration of reactants[27–30]. Herein, we reported systematic study on rapid synthesis of stable AuNPs using citric acid (CA), dihydrolipoic acid (DHLA, 6,8-dimercaptooctanoic acid) and DHLA-Alanine (DHLA-Ala) under the UV (311 nm) irradiation in less than 5 min (min). While CA is used as a reducing agent, DHLA and DHLA-Alanine act as strong stabilizing agents in synthesis of the Au NPs. We examined the formation of DHLA and DHLA-Ala capped AuNPs (DHLA@AuNPs and DHLA-Ala@AuNPs) as a function of the reaction time, pH of the reaction solution and reaction temperature. The stability of the AuNPs was also tested in varying salt concentrations and storage temperatures. 4-Nitrophenol is a toxic compound and can cause environmental contamination. The reduction of 4-nitrophenol to 4-aminophenol, which is used in the pharmaceutical industry, especially in the production of painkillers and antipyretics such as paracetamol (acetaminophen), allows the formation of an environmentally friendly material by converting this toxic compound into a less harmful substance. Carrying out this reduction reaction with a catalyst increases the speed and efficiency of the reaction[31]. The catalytic activity of the AuNPs was studied by conversion of 4-nitrophenol (4-NP) to 4-aminophenol (4-AP) in the presence of sodium borohydride in aqueous solution.

Experimental section

Materials Gold (III) chloride triydrate, 4- nitrophenol, sodium chloride (NaCl), hydrogen peroxide (H_2O_2), and lipoic acid were purchased from Sigma-Aldrich. Dihydrolipoic acid **2** and lipoylbenzotriazole **3** were prepared according to the previously reported procedure[32].

Instrumentation UV fluorescent narrow band lamp (Philips PL-S 2×9 W) with wavelength of 311 nm was used in the photoreductive Au-NP synthesis. The synthesised AuNPs were characterised by UV-Vis spectrophotometry (UV-Vis), scanning transmission electron microscopy (STEM), dynamic light scattering (DLS) and zeta potential (ZT) analysis.

Synthesis of capping ligands, dihidrolipoyl alanine (5, DHLA-Ala) *Coupling of lipoylbenzotriazole with amino acid.* Triethylamine (15 mmol) was added to the suspension of alanine (15 mmol) in water (6 mL) at 10 °C. A solution of lipoyl benzotriazole **3** (10 mmol) in 15 mL 1,4-dioxane was added to this solution dropwise, then it was stirred for 6 h at room temperature. The reaction was monitored with TLC using EtOAc/hexane (1:2) solution. After the reaction was completed, the excess amount of solution was removed, and then 40 mL of water was added to the remaining suspension. The solution was acidified by adding 4 N HCl to obtain pH 2–3. The solution was extracted with CH_2Cl_2 (3×20 mL). The collected organic phase was washed with 4 N HCl (3×10 mL) and saturated NaCl solution (10 mL) and dried over Na_2SO_4. The excess solvent was removed under reduced pressure to give lipoyl alanine (LA-Ala) as a light-yellow oil (70%) as a mixture of diastereomers. ^{1}H NMR (400 MHz, $CDCl_3$-*d*) *δ* (*diastereomeric mixture*) 7.60 (brs, 1 H), 6.17 (d, *J* = 6.8 Hz, 1 H), 4.62–4.50 (m, 1 H), 3.60–3.54 (m, 1 H), 3.26–3.02 (m, 2 H), 2.50–2.42 (m, 1 H), 2.32–2.20 (m, 2 H), 1.90–1.86 (m, 1 H), 1.70–1.60 (m, 4 H), 1.56–1.48 (m, 2 H), 1.46 (d, *J* = 7.1 Hz, 3 H).;^{13}C NMR (100 MHz, $CDCl_3$-*d*) (*diastereomeric mixture*) *δ* 175.9, 173.6, 56.4, 48.3, 40.3, 38.6, 36.2, 34.7 (34.6 *d*), 28.9 (28.8 *d*), 25.4 (25.3 *d*), 18.2.; HRMS: m/z $[M+H]^+$ calc. for $C_{11}H_{20}NO_3S_2^+$: 278.0879; found: 278.0883; $[M+Na]^+$ calc. for: $C_{11}H_{19}NNaO_3S_2^+$: 300,0699; found: 300.0706. Supporting Information (SI) with^{1}H NMR[13], C NMR, and HSQC NMR spectra of **5** (LA-Ala) were given in Fig. S1, S2 and S3.

Reduction of lipoyl amino acid, Lipoyl alanine (1 mmol) was dissolved in an aqueous solution of methanol (10 mL) and 0.25 M $NaHCO_3$ (5 mL). $NaBH_4$ (4 mmol) was slowly added to the mixture at 0 °C in an ice bath. The mixture was stirred for 1 h at 10 °C. The volatile part of the solution was removed under reduced pressure. The pH of solution was set to 2–3 by adding 4 N HCl. The solution was extracted with CH_2Cl_2 (3×10 mL). The organic phase was washed with saturated NaCl solution (10 mL) and dried over Na_2SO_4. The solvent was removed under reduced pressure to give dihydrolipoyl alanine (DHLA-Ala) as a colorless oil (90%) as a mixture of diastereomers. ^{1}H NMR (400 MHz, $CDCl_3$-*d*) *δ* (*diastereomeric mixture*) 8.17 (br s, 1 H), 6.25 (d, *J* = 6.9 Hz, 1 H), 4.70–4.50 (m,1 H), 2.94–2.80 (m, 1 H), 2.80–2.60 (m, 2 H), 2.30–2.20 (m, 2 H), 1.92–1.54 (m, 8 H), 1.45 (d, *J* = 6.0 Hz, 3 H), 1.40–1.28 (m, 2 H);^{13}C NMR (100 MHz, $CDCl_3$-*d*) *δ* 176.3, 173.8, 48.4, 42.9, 39.4, 38.8, 36.3, 26.6, 25.3, 22.4, 18.2.; HRMS: m/z $[M+H]^+$ calc. for $C_{11}H_{22}NO_3S_2^+$: 280.1036; found: 280.1041. Figure 1. shows the synthesis of dihydrolipoic acid (DHLA) and DHLA-Alanine (DHLA-Ala)[1]. H NMR[13], C NMR, and HSQC NMR spectra of **6** (DHLA-Ala) were shown in Fig. S4, S5 and S6.

Synthesis and characterization DHLA@AuNPs and DHLA-Ala@AuNPs First, 0.1 mM CA and 0,5 mM of 0.25 mL DHLA dissolved in ethanol solutions were added into 1 mL of 0,5 mM Au^{+3} solution. This mixture was exposed to UV irradiation under mild-stirring, then a color change from transparent to red-purple color as indication of the AuNP formation was observed in different type periods. In order to stop the reaction and remove any unreacted components, the Au NP solutions were centrifuged at 12.000 rpm for 15 min (min) for at

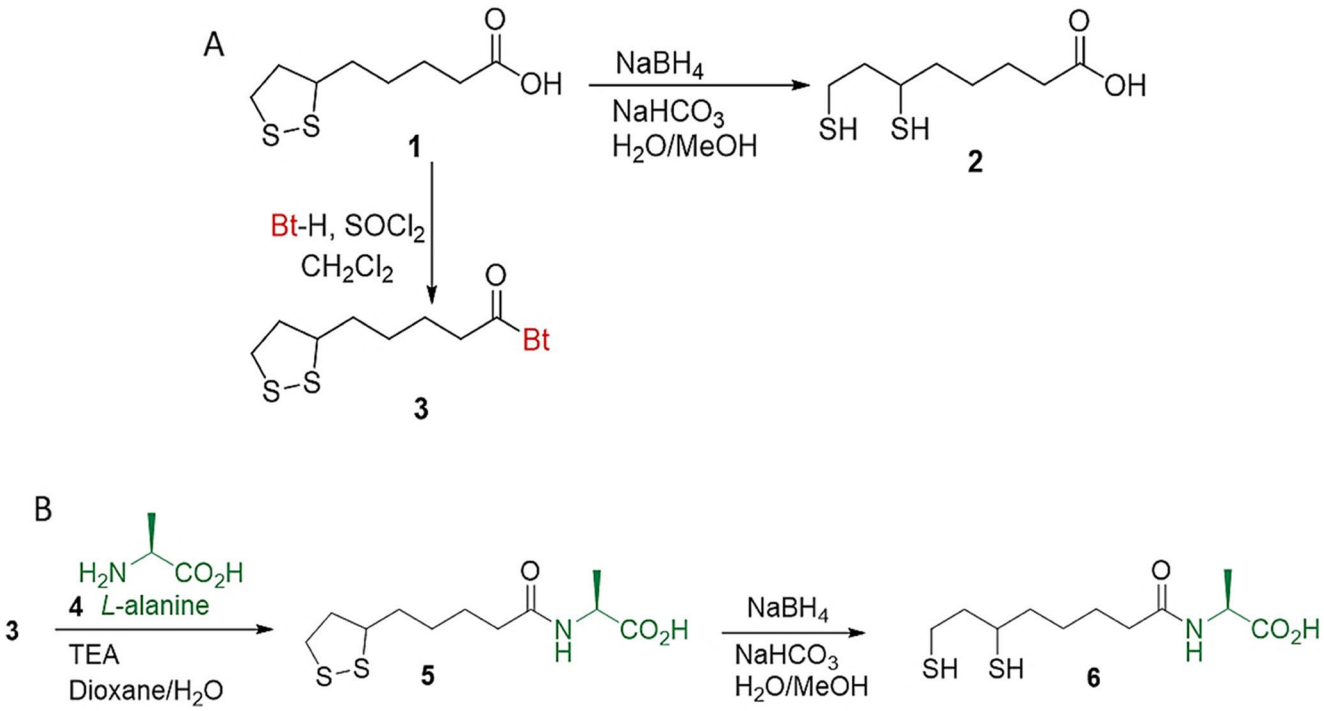

Figure 1. Synthesis of DHLA and DHLA-Ala.

least twice. The synthesized AuNPs were stored at 4 °C for characterization and activity experiment. In terms of characterization, the absorbance peaks, morphologies, hydrodynamic sizes and surface charges of both DHLA@AuNPs and DHLA-Ala@AuNPs were determined by UV-Vis spectrophotometer (UV-Vis), Scanning transmission electron microscope (STEM), dynamic light scattering (DLS) and Zeta potential (ZT), respectively. The same experimental procedure and characterization methods were followed to synthesize DHLA-Ala@AuNP and elucidate its structure, respectively.

Catalytic activity of DHLA@AuNPs and DHLA-Ala@AuNPs The reduction of 4-nitrophenol (4-NP) to 4-aminophenol (4-AP). Briefly, 2 mL of 0.2 mM 4-NP solution prepared and mixed 12 mM sodium borohydride ($NaBH_4$) at room temperature (RT: 25 °C)[33], then, 0.5 mL DHLA-AuNPs and DHLA-Ala@AuNPs solutions were separately added into each mixture. Finally, the reduction of 4-NP to 4-AP was recorded by UV-Vis.

Results and discussion

Synthesis and characterization DHLA@AuNPs and DHLA-Ala@AuNPs Although the conventional thermal reduction method using trisodium citrate as both reducing and capping agent is well documented for the synthesis of AuNPs, these AuNPs may not be synthesized in positioning form owing to high local temperature and they have tendency to aggregate in mid concentration of salt solution due to detachment of citrate molecules. The light-drive photoreduction methods are noninvasive and able to create AuNPs in targeted position at 25 °C. For instance, Scaiano and co-workers proposed the photochemical synthesis of AuNPs with photoinitiator molecules without using any stabilizing agents. These photoinitiators produce acetone ketyl radicals through Norrish-Type-I R-cleavage mechanism under the UV light, which act as reducing agents and induce the reduction of Au^{3+} to Au^{2+} and to Au^{1+}, eventually zero-valance Au^0 state to form AuNPs[28]. However, these unprotected AuNPs are prone to aggregation against small changes in pH and salt concentration of aqueous solution. Several other photoreduction methods may require some expensive reagents and long UV exposure time[29,34].

Herein, we report a rapid and photochemical synthesis of stable Au NPs using CA, DHLA and DHLA-Ala. We used CA as a potential reducing agent to accelerate generation of Au0. CA molecules only show weak adsorption onto Au NP, then cannot be efficiently used as a stabilizing agent in Au NP synthesis. However, DHLA and DHLA-Ala both acts as stabilizing agents due to their bidentate feature to form stable DHLA and DHLA-Ala capped gold nanoparticles (DHLA@Au NPs and DHLA-Ala@Au NPs). It is worth to note that while the oxidized (disulfide) form of lipoic acid (LA) needs much reaction time to bind surface of the AuNPs, reduced (di-thiol) LA called "dihydro-lipoic acid, DHLA) and its derivatives preferentially and rapidly bind onto AuNPs via thiol – Au chemistry. We demonstrated that UV irradiation promoted DHLA which directed the Au NP formation was accomplished in situ by one step reaction. Using LA in DHLA form (reduced) provided much rapid the Au NP formation in one phase reaction owing to no need of homolytic cleavage of S – S bonds. Also, it has been known that the photoinduced reductions of Au^{3+} in the presence of biothiols are hampered by the strong interaction of the thiols with Au^{3+} that allows the formation of stable $[Au-thiol]^{m+}$ complexes.[35–37] Taking advantage of this, colorimetric detection of biological thiols can be done based on target-triggered

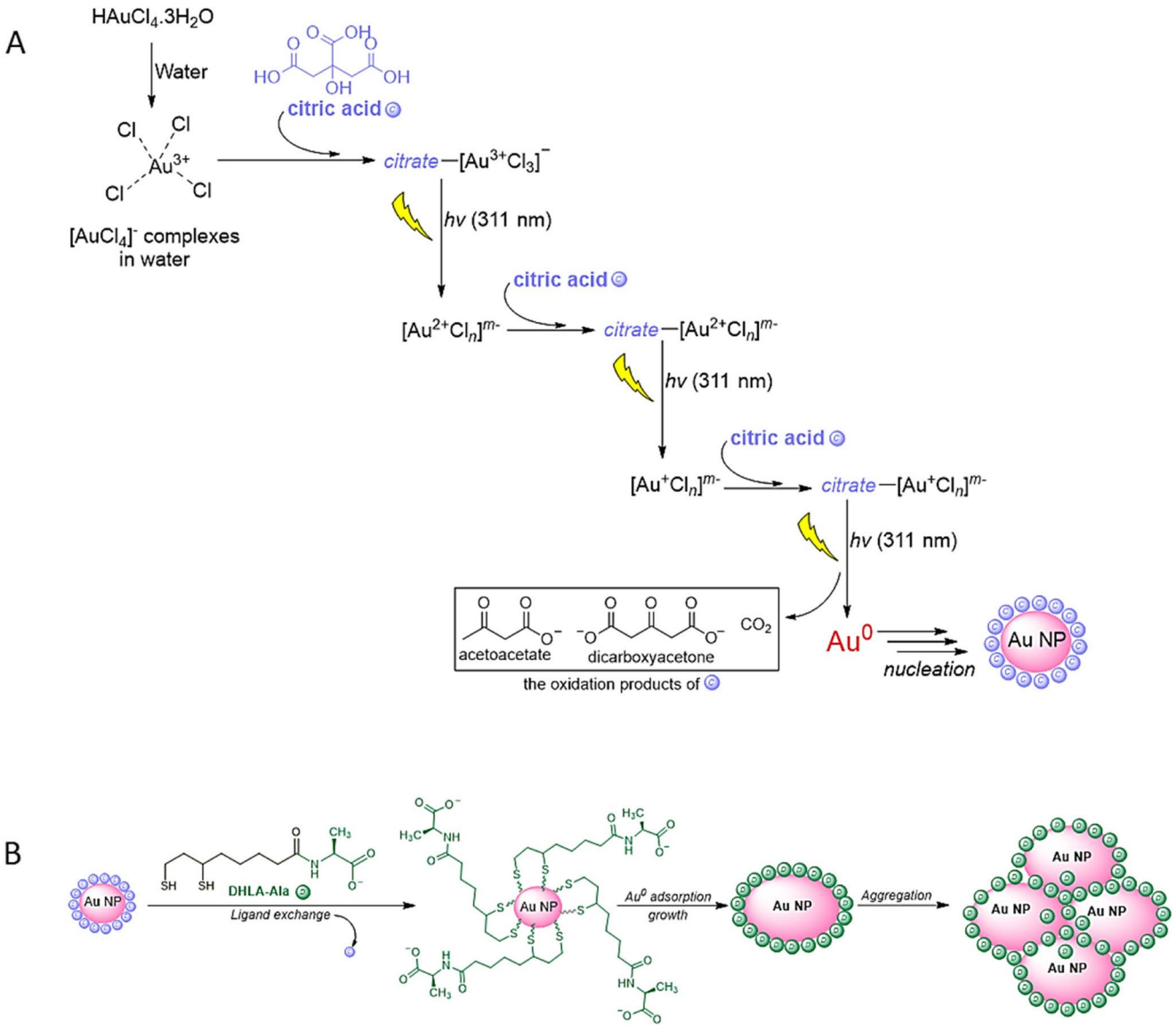

Scheme 1. Plausible mechanism for the reduction of (**A**) Au^{3+} to Au^0 and (**B**) The formation of DHLA@Au NPs and DHLA-Ala@Au NPs.

inhibition of photoinduced formation of AuNPs[35]. Although the presence of biothiols prevents the formation of AuNPs under light, Au NPs can be obtained by adding reductants with chelating and reducing properties, such as citric acid[36]. Shiraishi et al. previously proposed a mechanism for the formation of AuNPs[38]. They suggested that consecutive photoexcitation of citrate–$AuCl_n^{m-}$ complexes led to the reduction of Au^{3+} to Au^0, while citric acid was oxidized under 254 nm light irradiation from a Xe lamp. Subsequent analysis revealed the formation of carbon dioxide, acetoacetate, and dicarboxyacetone as the oxidation products of citric acid. Scheme shows the reduction of Au^{3+} to Au^0 in the presence of CA and the formation stable of DHLA@Au NPs and DHLA-Ala@Au NPs after a rapid in situ ligand exchange.

In the initial stage of the reaction, citrate binds to Au^{3+} cations and reduces them to Au^0 nuclei through electron transfer, aided by UV irradiation. As the photo-irradiation reaction proceeds, the concentrations of citrate and Au cations decrease. Once elemental Au^0 zero valance are formed, a ligand exchange takes place, facilitated by the reduced CA concentration and the strong binding of thiol groups to the Au^0 nuclei. Subsequent adsorption of Au^0 onto these nuclei promotes the growth of AuNPs. Citrate anions and newly exchanged DHLA that adhere to the AuNP surface act as stabilizing reagents, preventing aggregation of AuNPs by means of electrostatic repulsion.

We examined role of CA + DHLA-Ala, CA + DHLA and only CA for synthesis of the AuNPs as shown in Fig. 2. For synthesis of all AuNPs, concentration of each component was kept constant (0.5 mM Au^{3+}, 0.1 mM CA and 0.5 mM DHLA-Ala and 0.5 mM DHLA). The reactions for all AuNPs formation was performed at pH 2,4. For instance, 0.1 mM CA and 0.5 mM DHLA-Ala solutions were added into 1 mL of 0.5 mM Au^{3+} solution freshly prepared in deionized water. The resultant transparent mixture was exposed the UV irritation for

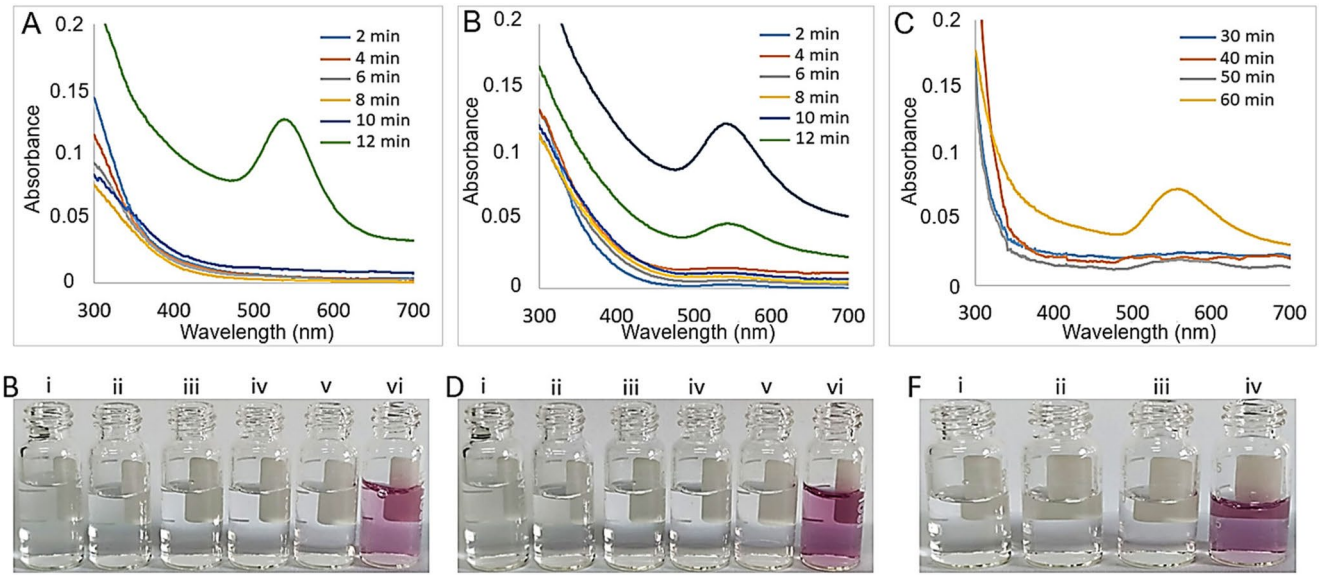

Figure 2. Time dependent formation of AuNPs. (**A**-**B**) UV-Vis spectrum and solution color of DHLA-Ala@AuNP. (**C**-**D**) UV-Vis spectrum and solution color of DHLA@AuNP and (**E**-**F**) UV-Vis spectrum and solution color of only CA@AuNP.

different time periods under mild-stirring to form DHLA-Ala@AuNPs. The characteristic absorbance peak and solution color of the AuNPs were both recorded at 12. min of reaction with 535 nm (green line) and light reddish color as shown in Fig. 2A and B (vi), respectively, both of which can be indication of synthesized DHLA-Ala@AuNPs. While the absorbance peaks of the mixture were ranging of 260–280 nm, its color remained transparent till 12.min of reaction. Interestingly, although no distinct color was observed by the naked eye, the DHLA@AuNPs was formed in first 10 min of reaction as peaks recorded at 550 nm (blue line) due to the surface plasmon resonance of DHLA@AuNPs (Fig. 2C). However, light reddish color was clearly observed at 12. min of reaction (Fig. 2D (vi), which is supported by a sharp and intense absorbance peak appeared at 542 nm (green line). Literately, the CA capped AuNPs (CA@AuNPs) were also formed but the reaction required at least 60 min UV irradiation to see first absorbance peak (Fig. 2E) and light reddish color solution (2 F(iv)). This could indicate that while CA functions as an effective reductant, it is not preferable as a stabilizing agent owing to its weak adsorption onto AuNPs. We claim that CA needs additional stabilizing agent like DHLA or elevated temperature for rapid and stable AuNP formation.

The effects of pH values (pHs) on formation of DHLA-Ala@AuNPs was also studied. Synthesis of DHLA-Ala@AuNPs was completed in 2 min at pH 11,5. Figure 3A shows that the absorbance peak of DHLA-Ala@AuNPs on UV spectrum was recorded at around 525 nm in 2. min of reaction (light blue line), which is also quite consistent with light-reddish color of the AuNP solution (Fig. 3B (i)) turned from transparent color (Fig. 3B). In contrast to alkaline condition, DHLA-Ala@AuNPs were not formed till 8.min of reaction at neutral pH (pH:7,2). A broad absorbance peak at 545 nm (yellow line), and slightly light red-purple color were seen after 8 min UV irradiation as demonstrated in Fig. 3C and D (iv).

It is known that alanine (Ala) is a nonpolar and aliphatic amino acid. The isoelectric point (Ip) of Ala in free form is around 6,02, where is amino group of Ala is protonated ($NH^{3+)}$) and its carboxyl group (COO-) is deprotonated at the same time, then zwitterion was formed with no net charge. While Ala is predominantly found in protonated (NH_3^+) form, its deprotonated forms (NH_2 and COO^-) exist in alkaline condition. It is worthy to mention that pKa values of carboxyl group and amino group of Ala are 2,35 (pKa1) and 9,87 (pKa2), respectively. Ala is in zwitterion forms with different degrees between pH 2,35 to 9,87. It is noted that carboxyl group of Ala is deprotonated when pH is above pKa1 and its amino group is in protonation when pH less than pKa2. In this study, we synthesized DHLA-Ala@AuNPs (in the presence of CA and DHLA-Ala) at original reaction pH (pH 2,4) in the synthesis protocol. The reduction of DHLA-Ala- $Au^{3+}Cl^{4-}$ complexes was complete to form DHLA-Ala@AuNPs in 2 min because DHLA-Ala ligand slightly undergoes deprotonation. The reaction pH was increased by addition of NaOH, then while DHLA-Ala@AuNP was formed in 2 min at pH 11,5 owing to highly deprotonated carboxyl group of Ala, which promotes the rapid Au^{3+} photoreduction, but DHLA-Ala@AuNP is synthesized in 8 min due to moderate deprotonation and predominant zwitterion form of Ala.

Our results show that the DHLA@AuNPs was formed in 2 min at pH 11,5, but absorbance peak is very broad and weak appeared at 557 nm (light blue line). Although the reaction was continued during 12 min for synthesis of DHLA@AuNPs, absorbance peaks were still considerably broad at around 550 nm (green line) (Fig. 4A). We believe that weak and broad absorbance peaks may reflect inefficient formation of the DHLA@AuNPs (low concentration) and relatively large size distribution. The pale color of DHLA@Au NPs solutions is attributed to low yield of synthesized DHLA@Au NPs (Fig. 4B). In addition to that, synthesis profile of DHLA@AuNPs is

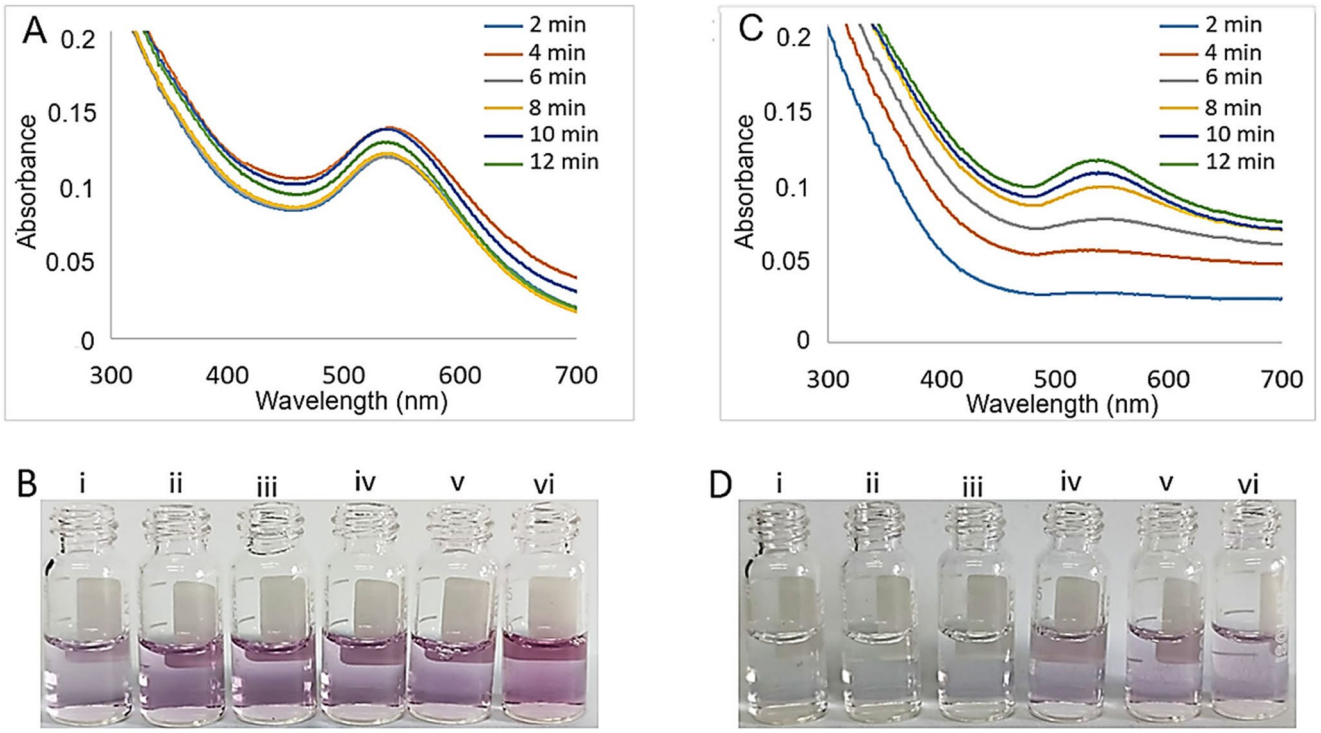

Figure 3. Time dependent formation of AuNPs at pH 11,5 and 7,2. (**A**-**B**) UV-Vis spectrum and solution color of DHLA-Ala@AuNPs at pH 11,5. (**C**-**D**) UV-vis spectrum and solution color of DHLA-Ala@AuNPs at pH 7,2.

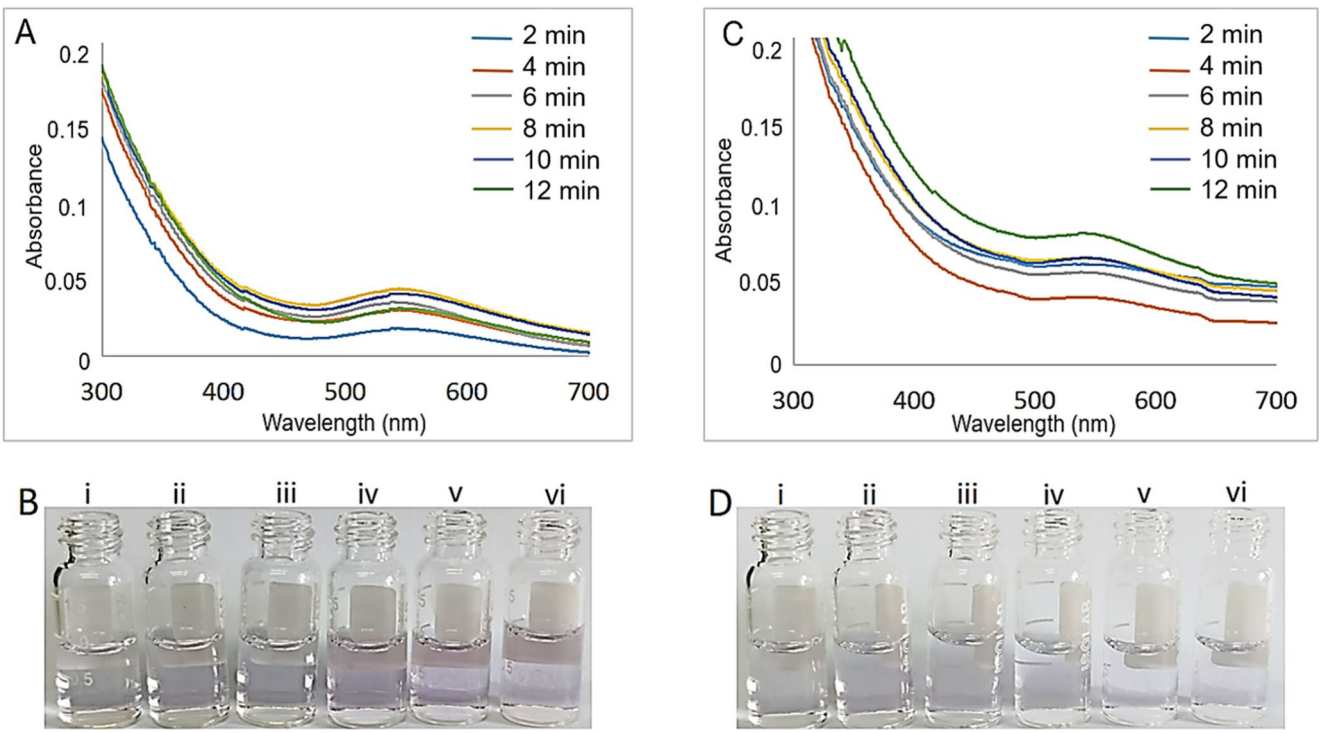

Figure 4. Time dependent formation of Au NPs at pH 11,5 and 7,2. (**A**-**B**) UV-vis spectrum and solution color of DHLA@AuNP at pH 11,5. (**C**-**D**) UV-Vis spectrum and solution color of DHLA@AuNP at pH 7,2.

similar to DHLA-Ala@Au NPs synthesis at neutral pH (pH:7,2) because the DHLA@Au NPs were not properly formed based upon UV spectrum and color of DHLA@AuNPs solutions as given in Fig. 4C and D, respectively.

The colloidal form of the AuNPs in experimental parameters which is referred as "stable AuNPs" is an indispensable feature, which makes them available to use in scientific application. Otherwise, AuNPs in aggregated form cannot maintain their physicochemical, electronic and biological properties. As a further study, stability of the AuNPs produced by citrate, DHLA-Ala and DHLA molecules were tested against different concentration of sodium chloride (NaCl) salt solutions. For instance, although citrate reduction at boiling point is the most established and common method for synthesis of citrate capped AuNPs, citrate molecules on surface of the AuNP easily and rapidly detaches with increased NaCl concentration. Figure 5 reveals that the characteristic absorbance peak of colloidal citrate capped AuNPs at 525 nm (Fig. 5A) and its wine-red color (Fig. 5D) remained unchanged till 50 mM NaCl solution. However, AuNPs aggregation initiated when the NaCl concentration reached 50 mM, which was confirmed with distortion in UV spectrum from narrow and sharp peaks recorded at 525 nm to very broad peaks at seen between 560 and 720 nm. Additionally, aggregation caused the wine-red color of AuNP solution to turn blue-purple in 50 mM and above NaCl solution due to changes in refractive index of AuNP solution.

However, DHLA-Ala@AuNPs and DHLA@AuNPs showed enhanced tolerance against even high concentration of NaCl solution (200 mM). While initial absorbance peak appeared at 535 nm (Fig. 5B) and reddish color (Fig. 5E) of DHLA-Ala@AuNPs moved to 550 nm (Fig. 5C) and slight purplish (Fig. 5F), respectively, absorbance peak of DHLA@AuNP at 542 nm and its reddish color shifted to 575 nm and purplish in a manner. Conversion of the reddish color to purplish might be getting closer proximity of the AuNPs each other in solution but which did not create any remarkable distortions on UV-Vis spectra. We conclude that high stability of DHLA-Ala@AuNPs and DHLA@AuNPs in even 200 mM NaCl solution can be attributed to strong interaction of Au − S bonds and then no detachment of thiolate in DHLA ligands.

Furthermore, we also investigated how storage temperatures like + 4 °C and 25 °C influence stability of the pre-synthesized AuNPs (Fig. 6). The DHLA-Ala@AuNPs and DHLA@AuNPs were stored at + 4 °C (Fig. 6A and C) and at 25 °C (Fig. 6B and D) for 7 days, no changes on UV spectra and in solution color for each AuNP were observed. Although both DHLA-Ala@AuNPs and DHLA@AuNPs were stored at 25 °C for 30 days, they maintained their stabilities without any aggregation or precipitation (data now shown here). These findings strongly support our explanation of strong interaction between thiolate groups of DHLA ligands and Au surface. Conversely, while CA@AuNPs are somewhat stable at + 4 °C (Fig. 6E), they completely decomposed at 25 °C even for 1-day incubation (Fig. 6E). CA@NPs lost its intrinsic absorbance peak and reddish color at 25 °C, both of which revealed that CA can be a potential reductant to reduce Au^{3+} to Au^{0} for synthesis of AuNPs, but it is not an ideal capping agent to produce stable AuNPs.

The DHLA-Ala@AuNPs were synthesized at different temperatures (40 °C, 60 °C and 80 °C) to elucidate the role of reaction temperature in situ synthesis of the AuNPs (Fig. 7). Firstly, the DHLA-Ala@AuNPs was successfully synthesized at 25 °C via 12 min UV irritation as shown in Fig. 2A, but we demonstrated that DHLA-Ala@AuNPs were formed much faster at elevated temperature due to complementary thermal reduction process. First absorbance peak at 548 nm (yellow line) (Fig. 7A) and reddish color (Fig. 7B) of DHLA-Ala@AuNPs appeared in 6 min at 40 °C. The synthesis of DHLA-Ala@AuNPs started in 2 min at 60 °C but more district peak at 568 nm (grey line) was recorded in 4 min with light reddish color (Fig. 7C and D). At 80 °C, DHLA-Ala@AuNPs gave the first clear and acceptable absorbance peak at 568 nm (light blue line) with also reddish color in

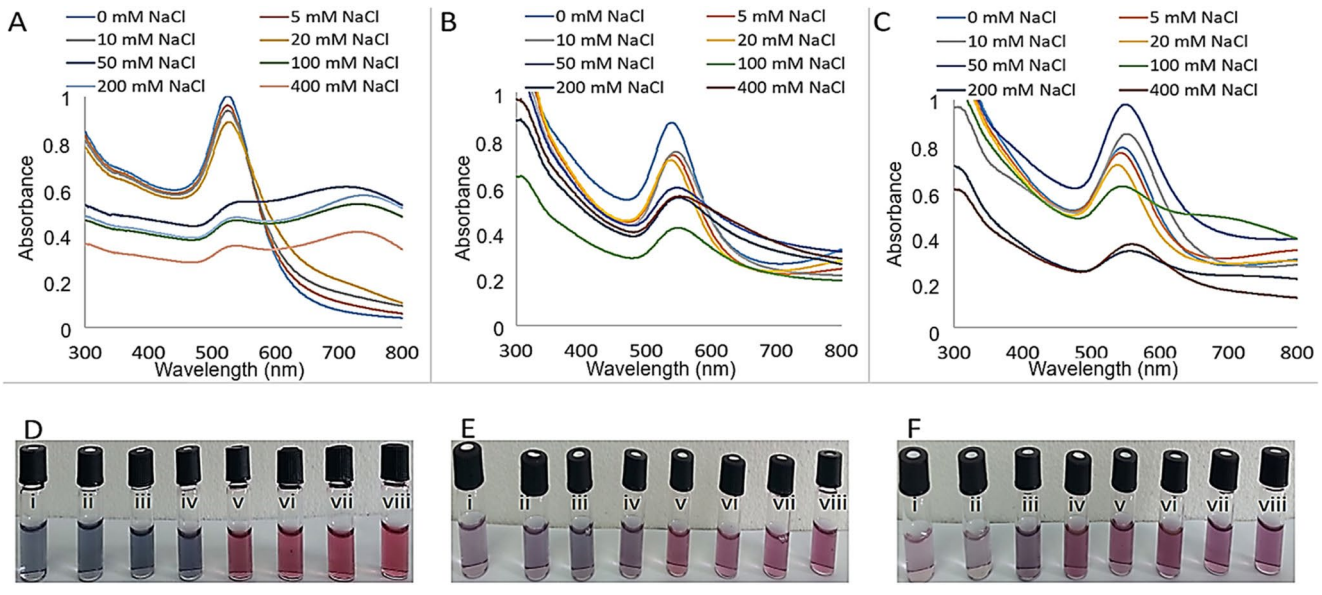

Figure 5. Stability of Au NPs in the presence of different concentrations of salt (NaCl) solutions. (**A**-**D**) DHLA-Ala@AuNPs, (**B**-**E**) DHLA@AuNPs and (**C**-**F**) citrate capped AuNPs.

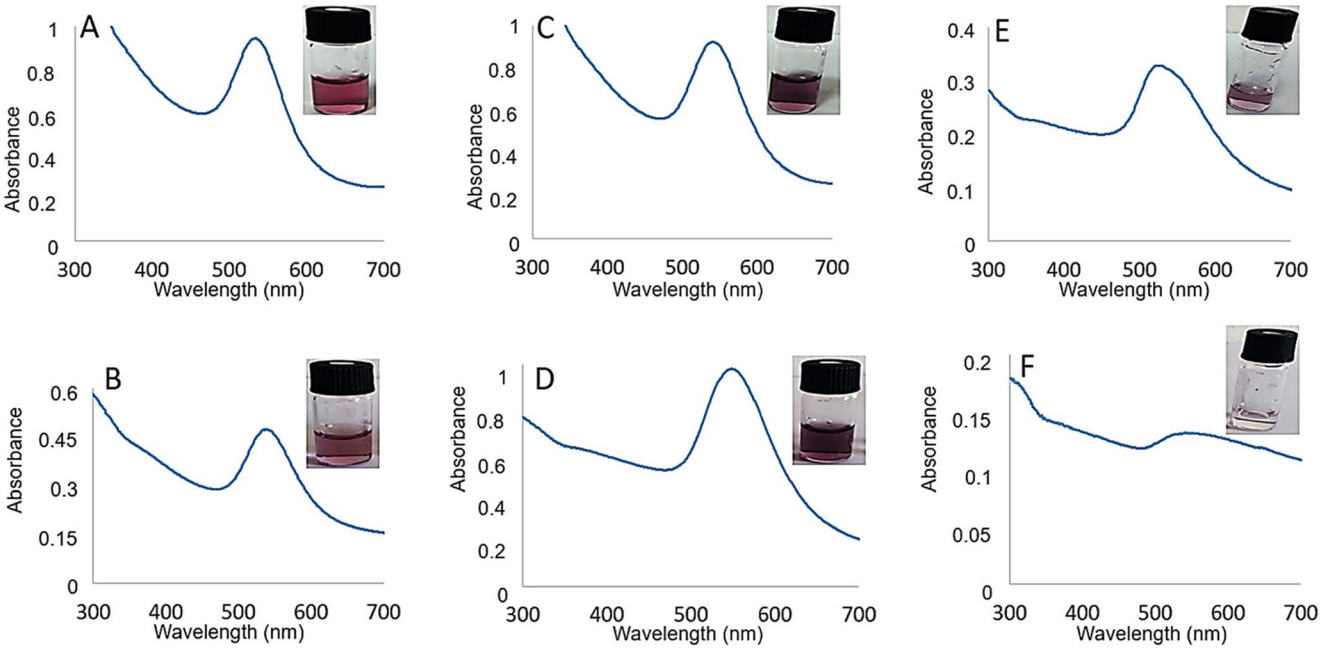

Figure 6. Stability of AuNPs at 25 °C form by (**A**-**B**) CA + DHLA-Ala, (**C**-**D**) CA + DHLA and (**E**-**F**) only CA.

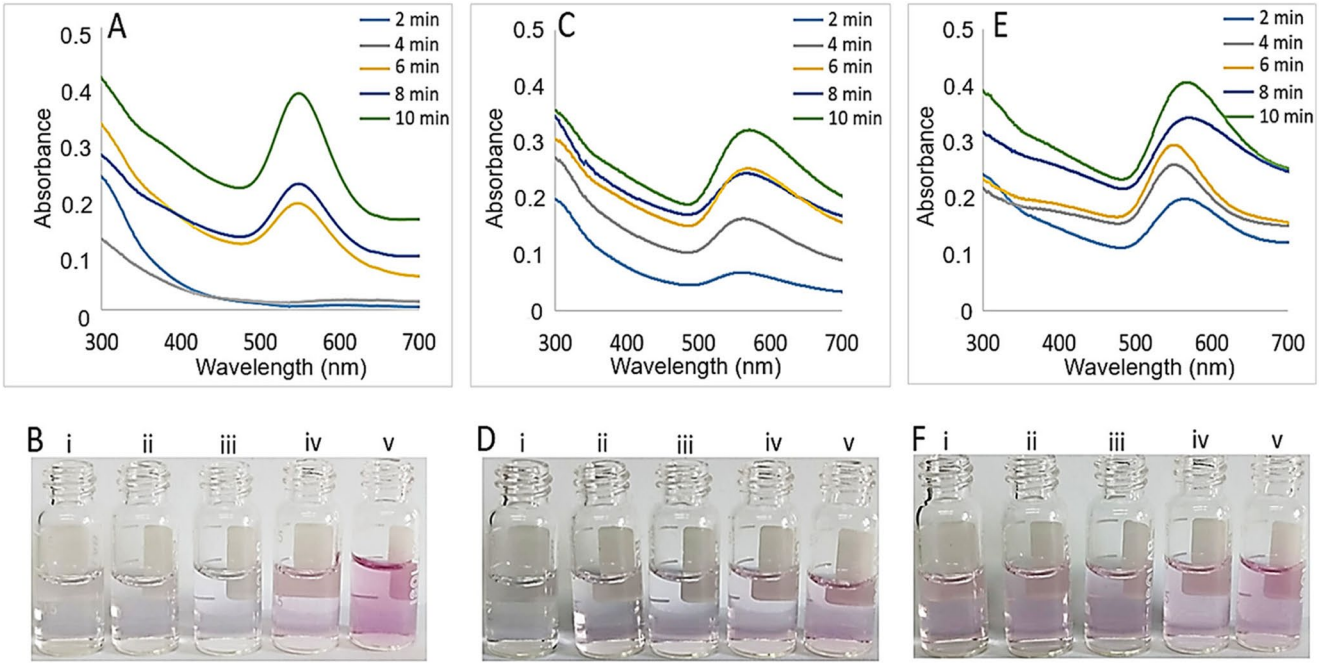

Figure 7. Synthesis of DHLA-Ala@AuNPs at different temperatures. (**A**-**B**) 40 °C, (**C**-**D**) 60 °C and (**E**-**F**) 80 °C.

2 min (Fig. 7E and F). The thermal aggregation occurring at any given temperature can indicate the DHLA-Ala@AuNPs stability. For instance, while no distortion was seen on UV spectra and absorbance peaks of DHLA-Ala@AuNPs were kept between 562 nm 578 nm, we observed a change in the reddish color of DHLA-Ala@AuNP solutions. In literature, thermal reduction usually triggers thermal aggregation which is associated with weak adsorption and/or desorption of reducing or capping onto the AuNPs surface[27].

Temperature dependence of in situ synthesis of DHLA@AuNPs was investigated at different temperatures for DHLA-Ala@AuNPs as shown in Fig. 7. The DHLA@AuNPs was formed at both 25 °C and 40 °C in 10 min of reaction. However, formation of DHLA@AuNPs at 40 °C in 10 min was supported by both absorbance peaks at 542 nm (green line) (Fig. 8A) and light reddish color (Fig. 8B). The DHLA@AuNPs were first formed in

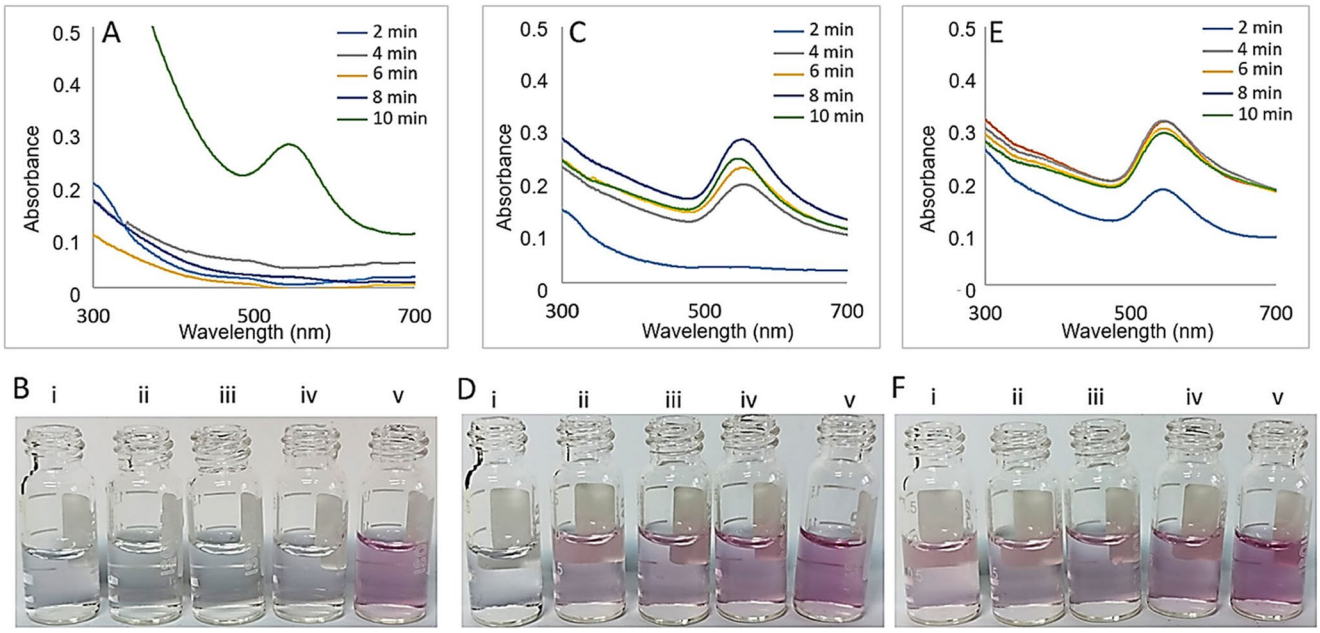

Figure 8. Synthesis of DHLA@AuNPs at different temperatures. (**A**-**B**) 40 °C, (**C**-**D**) 60 °C and (**E**-**F**) 80 °C.

2 min at 60 °C. The absorbance peak appeared at 539 nm (yellow line) is quite narrow and clear (Fig. 8C) and it is consistent with corresponding color (Fig. 8D). The initial formation of DHLA@AuNPs started at 80 °C in 2 min as absorbance peak was observed at 548 nm (light blue line) (Fig. 8E) and pale reddish color appeared (Fig. 8F). The reason for the rapid formation of DHLA@AuNPs at elevated temperatures can be explained by the contribution of thermal reduction. Although desorption of CA is expected at elevated temperatures, DHLA@AuNPs is still considered quite stable owing to strong interaction between thiol group of DHLA and Au surface.

Morphologies of the AuNPs were monitored with STEM images. The DHLA-Ala@AuNPs have spherical shape with size of 9 nm ± 2 (Fig. 9A). These Au NPs are quite monodispersed and uniform, and they did not show any aggregation after being left at 25 °C for 7 days (Fig. 9B). Size of DHLA@AuNPs was measured to be 15 nm ± 2 with spherical shapes (Fig. 9C). Like DHLA-Ala@AuNPs, DHLA@AuNPs were also quite stable after 7 days of incubation at 25 °C since no large-scale aggregation was observed in a STEM image (Fig. 9D). In addition to that, while CA-capped AuNPs are spherical and monodispersed with size of around 6 nm (Fig. 9E) expectedly, they aggregated even after being stored 1 day at 25 °C as shown in the STEM image of Fig. 9F.

As a further characterization, the surface charge and hydrodynamic size of each synthesized AuNPs were measured before and after 25 °C incubation (Fig. 10). Before incubation of all AuNPs at 25 °C, surface charge and effective dimeters for DHLA-Ala@AuNPs (Fig. 10A and B), DHLA@AuNPs (Fig. 10C and D), and CA@AuNP (Fig. 10E and F) were determined to be – 41 mV and 30 nm, – 25 mV and 40 nm and – 41 mV and between 30 nm and 250 nm, respectively. After the AuNPs were incubated at 25 °C, surface charge and effective dimeters for DHLA-Ala@AuNPs (Fig. 10G and H), DHLA@AuNPs (Fig. 10I and J), and CA@AuNP (Fig. 10K and L) were determined to be – 40 mV and 36 nm, – 26 mV and 45 nm and – 5 mV and 550 nm, respectively. All data of ZT and DLS are consistent with UV-Vis spectra, photos of the solution, and STEM images of the AuNPs.

Our results demonstrate that there are no remarkable differences in ZT and DLS data of DHLA-Ala@AuNPs and DHLA@AuNPs before and after 25 °C incubation owing to strong binding between thiol groups of DHLA ligands and Au surface. This suggests that no detachment of DHLA ligands from Au surface occurred. In contrast, CA molecules are easily desorbed from Au surface, which induced the differences in ZT and DLS data of CA@AuNPs before and after 25 °C incubation.

The catalytic properties of the DHLA-Ala@AuNPs and DHLA@AuNPs were evaluated via the reduction of 4-nitrophenol (4-NP) in the presence of sodium borohydride (NaBH4) to 4-aminophenol (4-AP) by following standard reaction as illustrated in Figs. 11[33,39–41]. Briefly, the 4-NP dissolved in water was mixed with $NaBH_4$, and then yellow color nitrophenolate anion solution was formed with a characteristic absorbance peak at 400 nm. The reduction of 4-NP molecules/nitrophenolate anions were catalyzed by the AuNPs, then the decrease in peak of 4-NP at 400 nm and increase in peaks of 4-AP at 300 nm were simultaneously observed as an indication of the conversion of 4-NP to 4-AP. Both DHLA-Ala@AuNPs (Fig. 11A) and DHLA@AuNPs (Fig. 11B) successfully catalyzed 4-NP to 4-AP, but DHLA@AuNPs much rapidly catalyzed 4-NP to 4-AP compared to DHLA-Ala@AuNPs, which might be due to higher number of active atoms or active sites in Au NPs for catalysis. The substrate-like 4-NP may not get the right position or proper proximity on the surface of the AuNP owing to the steric and electrostatic effect of the DHLA-Ala ligand, then reduction of 4-NP to 4-AP which is catalyzed by DHLA-Ala@AuNPs can be slower than DHLA@AuNPs. We believe that DHLA ligand makes 4-NP accessible to the active site of DHLA@AuNPs. The reaction kinetics for the reduction of 4-NP to 4-AP was carried out according to the

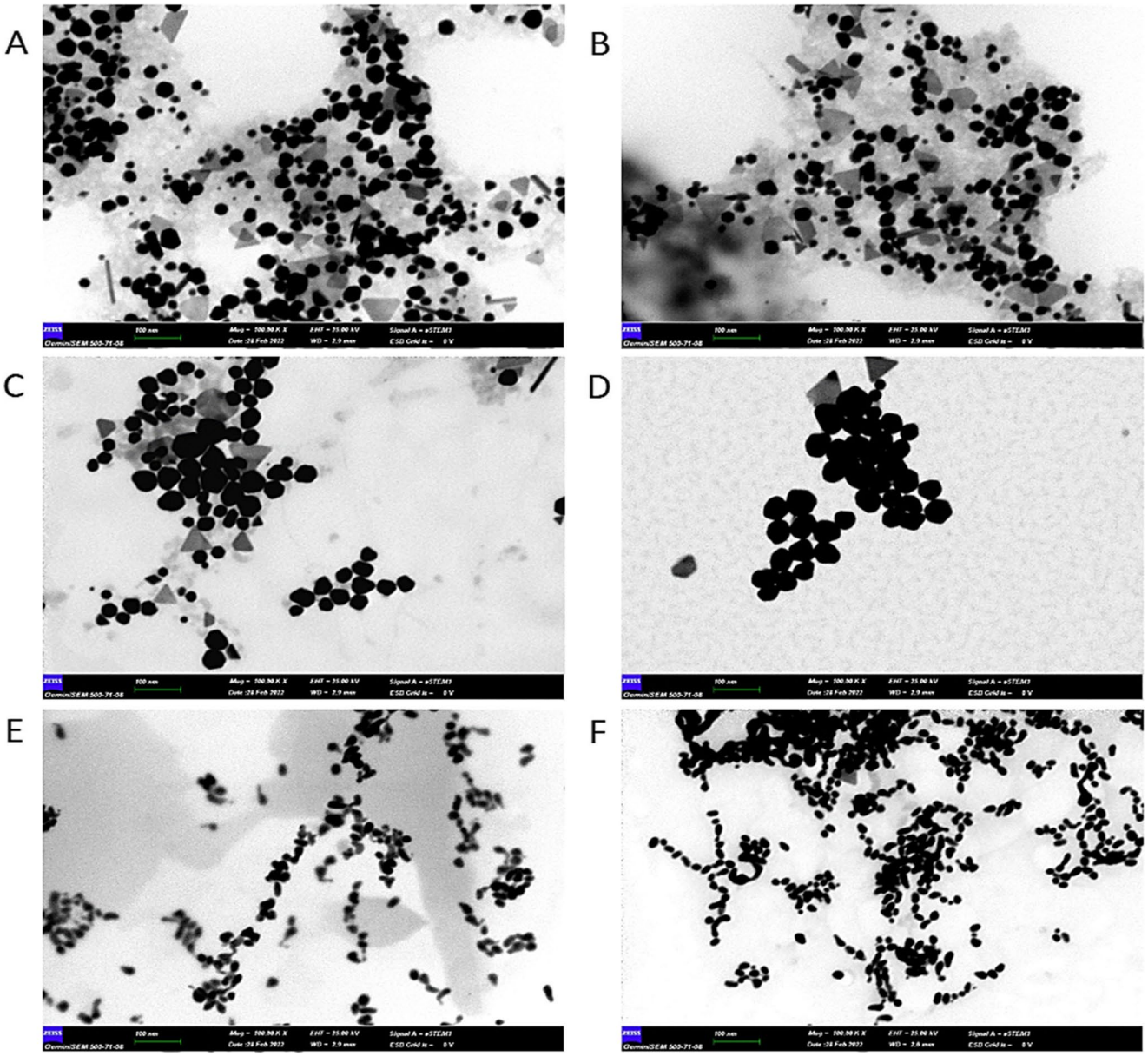

Figure 9. STEM images of the AuNPs. (**A**-**B**) DHLA-Ala@AuNPs before and after incubated at 25 °C, (**C**-**D**) DHLA@AuNPs before and after incubated at 25 °C and (**E**-**F**) CA@AuNPs before and after incubated at 25 °C. We run STEM with a 100 nm scale, 100.00 KX magnification and 25 kV.

method previously reported study[42]. Briley, k is the rate constant, C_0 is the initial concentration of 4-NP and C_t is the concentration of 4-NP at time 't'. The plots of -kt = ln(Ct/C0) under AuNP catalysis are shown in Fig. 11D.

Conclusion

We proposed a novel method for synthesis of stable AuNPs. The aqueous solution containing $HAuCl_4$ precursor and CA, DHLA, and DHLA ligands was exposed to UV (311 nm) irradiation at RT, then quite stable AuNPs, DHLA-Ala@AuNPs and DHLA@AuNPs, were formed in a short time (around 10 min). In the AuNPs synthesis, while CA acts as a reductant for both reduction of Au^{3+} to Au^0 and formation of the AuNPs, DHLA and DHLA-Ala ligands are utilized as stabilizing agents by strongly binding onto AuNPs through reduced (di-thiol) group owing to thiol – Au chemistry. Then, DHLA and DHLA-Ala ligands suppressed aggregation of the formed the AuNPs (DHLA-Ala@AuNPs and DHLA@AuNPs) against RT storage and high concentrated salt solutions. We run catalysis performance of DHLA-Ala@AuNPs and DHLA@AuNPs for conversion of 4-NP to 4-AP as a piece of application. We claim that based upon the results, this synthesis method is one step and simple to produce quite stable AuNPs at ambient condition in a short time. It may contribute to the synthesis of various metallic nanoparticles based on photoreduction strategy.

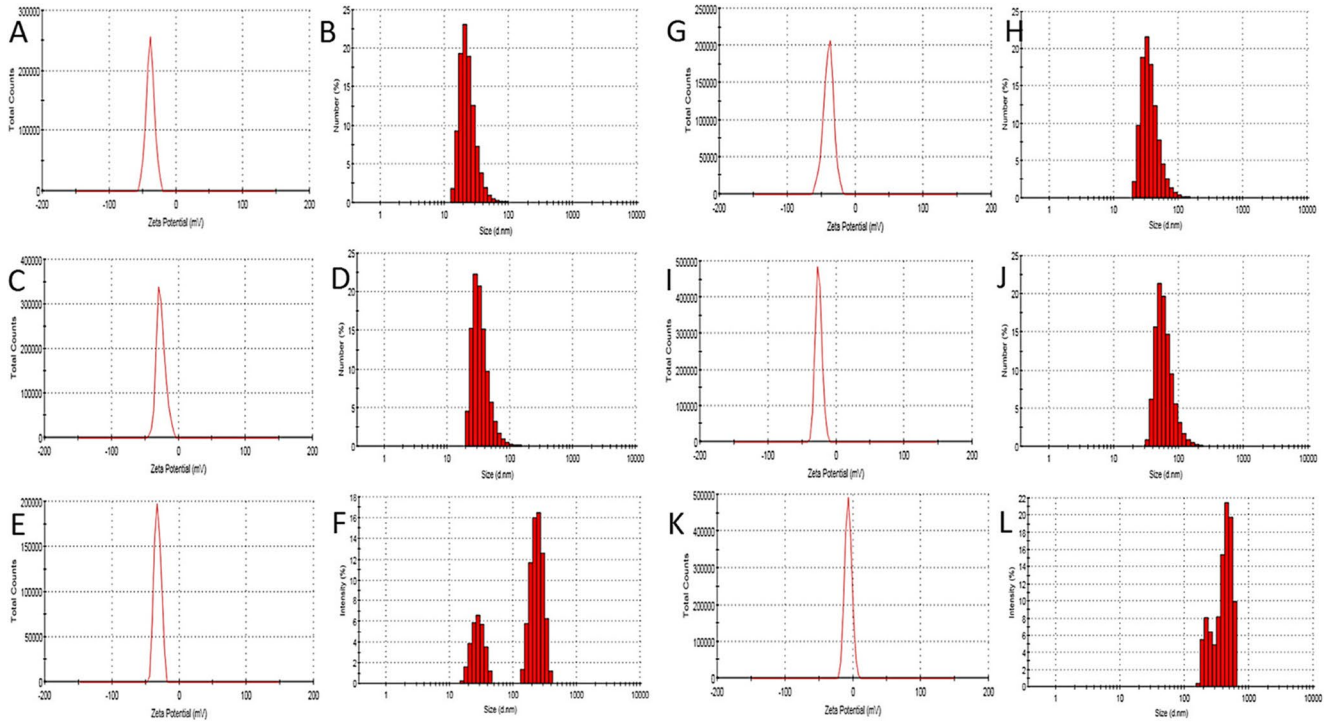

Figure 10. Zeta and DLS data of the AuNPs. A-B and G-J) DHLA-Ala@AuNPs before and after incubated at 25 °C. C-D and H-K) DHLA@AuNPs before and after incubated at 25 °C. E-F and I-L) CA@AuNPs before and after incubated at 25 °C.

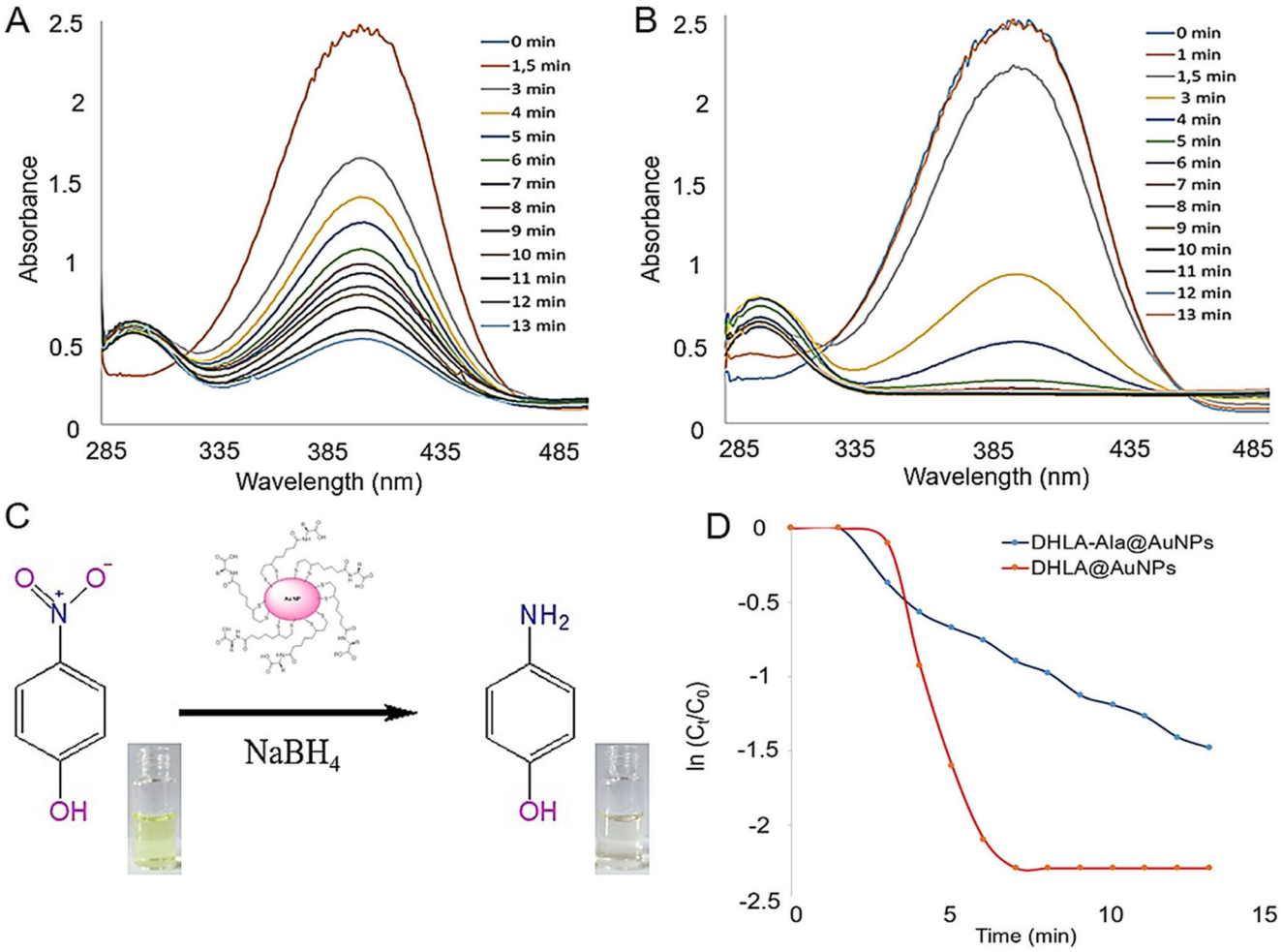

Figure 11. Reduction of 4-NP to 4-AP catalyzed by (**A**) DHLA-Ala@AuNPs and (**B**) DHLA@AuNPs (**C**) Chemical mechanism and color change of the reduction reaction (**D**) The plots of $-kt = \ln(C_t/C_0)$ of 4-NP reduction.

Data availability

"Most of the data generated or analysed during this study are included in this manuscript and in the supplementary information file. Other raw data are available from the corresponding author upon reasonable request".

Received: 15 May 2024; Accepted: 16 October 2024
Published online: 21 October 2024

References

1. Yeh, Y. C., Creran, B. & Rotello, V. M. Gold nanoparticles: preparation, properties, and applications in bionanotechnology. *Nanoscale*. **4** (6), 1871–1880 (2012).
2. Van de Looij, S. M. *et al*. Gold nanoclusters: imaging, therapy, and theranostic roles in biomedical applications. *Bioconjug. Chem.* **33** (1), 4–23 (2021).
3. Saha, K., Agasti, S. S., Kim, C., Li, X. & Rotello, V. M. Gold nanoparticles in chemical and biological sensing. *Chem. Rev.* **112** (5), 2739–2779 (2012).
4. Mieszawska, A. J., Mulder, W. J., Fayad, Z. A. & Cormode, D. P. Multifunctional gold nanoparticles for diagnosis and therapy of disease. *Mol. Pharm.* **10** (3), 831–847 (2013).
5. Cormode, D. P. *et al*. Nanocrystal core high-density lipoproteins: a multimodality contrast agent platform. *Nano Lett.* **8** (11), 3715–3723 (2008).
6. Kircher, M. F. *et al*. A brain tumor molecular imaging strategy using a new triple-modality MRI-photoacoustic-raman nanoparticle. *Nat. Med.* **18** (5), 829–834 (2012).
7. Manohar, S., Ungureanu, C. & Van Leeuwen, T. G. Gold nanorods as molecular contrast agents in photoacoustic imaging: the promises and the caveats. *Contrast Media Mol. Imaging*. **6** (5), 389–400 (2011).
8. Kumar, A. *et al*. Gold nanoparticles functionalized with therapeutic and targeted peptides for cancer treatment. *Biomaterials*. **33** (4), 1180–1189 (2012).
9. Qiu, L. *et al*. A cell-targeted, size-photocontrollable, nuclear-uptake nanodrug delivery system for drug-resistant cancer therapy. *Nano Lett.* **15** (1), 457–463 (2015).
10. Ocsoy, I. *et al*. DNA aptamer functionalized gold nanostructures for molecular recognition and photothermal inactivation of methicillin-resistant *Staphylococcus aureus*. *Colloids Surf., B*. **159**, 16–22 (2017).

11. Li, C. *et al*. Gold-coated Fe_3O_4 nanoroses with five unique functions for cancer cell targeting, imaging, and therapy. *Adv. Funct. Mater.* **24** (12), 1772–1780 (2014).
12. Yusufbeyoğlu, S. *et al*. The Use of Conjugated Gold Nanorods with reduced toxicity in Photothermal Therapy for MRSA. *ChemistrySelect*. **9** (11), e202304893 (2024).
13. Chen, T. *et al*. One-step facile surface engineering of hydrophobic nanocrystals with designer molecular recognition. *J. Am. Chem. Soc.* **134** (32), 13164–13167 (2012).
14. Yasun, E. *et al*. Enrichment and detection of rare proteins with aptamer-conjugated gold nanorods. *Anal. Chem.* **84** (14), 6008–6015 (2012).
15. Yasun, E. *et al*. Cancer cell sensing and therapy using affinity tag-conjugated gold nanorods. *Interface Focus*. **3** (3), 20130006 (2013).
16. Ocsoy, I. *et al*. Aptamer-conjugated multifunctional nanoflowers as a platform for targeting, capture, and detection in laser desorption ionization mass spectrometry. *ACS nano*. **7** (1), 417–427 (2013).
17. Shukoor, M. I. *et al*. Aptamer-nanoparticle assembly for logic-based detection. *ACS Appl. Mater. Interfaces*. **4** (6), 3007–3011 (2012).
18. Turek, D., Van Simaeys, D., Johnson, J., Ocsoy, I. & Tan, W. Molecular recognition of live methicillin-resistant *Staphylococcus aureus* cells using DNA aptamers. *World J. Translational Med.* **2** (3), 67 (2013).
19. Celik, C., Kalin, G., Cetinkaya, Z., Ildiz, N. & Ocsoy, I. Recent advances in Colorimetric tests for the detection of infectious diseases and Antimicrobial Resistance. *Diagnostics*. **13** (14), 2427 (2023).
20. Sezgin, G. C. *et al*. Development of a colorimetric urease test based on au NPs capped with anthocyanin for the Rapid Detection of Helicobacter pylori through multiple readouts. *ChemistrySelect*. **8** (27), e202300637 (2023).
21. Turkevich, J., Stevenson, P. C. & Hillier, J. A study of the nucleation and growth processes in the synthesis of colloidal gold. *Discuss. Faraday Soc.* **11**, 55–75 (1951).
22. Bajaj, M., Wangoo, N., Jain, D. V. S. & Sharma, R. K. Quantification of adsorbed and dangling citrate ions on gold nanoparticle surface using thermogravimetric analysis. *Sci. Rep.* **10** (1), 8213 (2020).
23. Wink, D. J. NSF outreach for teachers and students. *J. Chem. Educ.* **76** (7), 894 (1999).
24. Demirbas, A. *et al*. Synthesis of long-term stable gold nanoparticles benefiting from red raspberry (*Rubus idaeus*), strawberry (*Fragaria ananassa*), and blackberry (*Rubus fruticosus*) extracts–gold ion complexation and investigation of reaction conditions. *ACS Omega*. **4** (20), 18637–18644 (2019).
25. Unal, I. S., Demirbas, A., Onal, I., Ildiz, N. & Ocsoy, I. One step preparation of stable gold nanoparticle using red cabbage extracts under UV light and its catalytic activity. *J. Photochem. Photobiol., B*. **204**, 111800 (2020).
26. Lekeufack, D. D. & Brioude, A. One pot biosynthesis of gold NPs using red cabbage extracts. *Dalton Trans.* **41** (5), 1461–1464 (2012).
27. Shiraishi, Y. *et al*. Synthesis of au nanoparticles with benzoic acid as reductant and surface stabilizer promoted solely by UV light. *Langmuir*. **33** (48), 13797–13804 (2017).
28. McGilvray, K. L., Decan, M. R., Wang, D. & Scaiano, J. C. Facile photochemical synthesis of unprotected aqueous gold nanoparticles. *J. Am. Chem. Soc.* **128** (50), 15980–15981 (2006).
29. Harada, M. & Kizaki, S. Formation mechanism of gold nanoparticles synthesized by photoreduction in aqueous ethanol solutions of polymers using in situ quick scanning x-ray absorption fine structure and small-angle X-ray scattering. *Cryst. Growth. Des.* **16** (3), 1200–1212 (2016).
30. Ma, H. *et al*. Hot spots in photoreduced au nanoparticles on DNA scaffolds potent for robust and high-sensitive surface-enhanced Raman scattering substrates. *Mater. Chem. Phys.* **138** (2–3), 573–580 (2013).
31. Liu, K., Han, L., Zhuang, J. & Yang, D. P. Protein-directed gold nanoparticles with excellent catalytic activity for 4-nitrophenol reduction. *Mater. Sci. Engineering: C*. **78**, 429–434 (2017).
32. Avan, I., Nasirov, H., Kani, I. & Ozcan, A. ZnS/CuS nanocomposites: synthesis and catalytic activity on thymol oxidation. *J. Solgel Sci. Technol.* **107**, 149–160 (2023).
33. Peng, L. *et al*. Reversible phase transfer of nanoparticles based on photoswitchable host–guest chemistry. *Acs Nano*. **8** (3), 2555–2561 (2014).
34. Zhou, Y. *et al*. Regional selective construction of nano-Au on $F_{e3}O_4$@SiO_2@PEI nanoparticles by photoreduction. *Nanotechnology*. **27** (21), 215301 (2016).
35. Jung, Y. L., Park, J. H., Kim, M. I. & Park, H. GLabel-free colorimetric detection of biological thiols based on target-triggered inhibition of photoinduced formation of AuNPs. *Nanotechnology*. **27** (5), 055501 (2015).
36. Kostara, A., Tsogas, G. Z., Vlessidis, A. G. & Giokas, D. L. Generic assay of sulfur-containing compounds based on kinetics inhibition of gold nanoparticle photochemical growth. *ACS Omega*. **3** (12), 16831–16838 (2018).
37. Courrol, L. C., & de Matos, R. A. Synthesis of gold nanoparticles using amino acids by light irradiation. In *Catalytic application of nano-gold catalysts* (ed Mishra, N. K.) 83–99 (IntechOpen, 2016).
38. Shiraishi, Y., Tanaka, H., Sakamoto, H., Ichikawa, S. & Hirai, T. Photoreductive synthesis of monodispersed au nanoparticles with citric acid as reductant and surface stabilizing reagent. *RSC Adv.* **7** (11), 6187–6192 (2017).
39. Noël, S. *et al*. Catalytic reduction of 4-nitrophenol with gold nanoparticles stabilized by large-ring cyclodextrins. *New J. Chem.* **44** (48), 21007–21011 (2020).
40. Nigra, M. M., Ha, J. M. & Katz, A. Identification of site requirements for reduction of 4-nitrophenol using gold nanoparticle catalysts. *Catal. Sci. Technol.* **3** (11), 2976–2983 (2013).
41. Dadi, S., Temur, N., Gul, O. T., Yilmaz, V. & Ocsoy, I. In situ synthesis of horseradish peroxidase nanoflower@ carbon nanotube hybrid nanobiocatalysts with greatly enhanced catalytic activity. *Langmuir*. **39** (13), 4819–4828 (2023).
42. Rajamanikandan, R., Shanmugaraj, K. & Ilanchelian, M. Concentration dependent catalytic activity of glutathione coated silver nanoparticles for the reduction of 4-nitrophenol and organic dyes. *J. Cluster Sci.* **28**, 1009–1023 (2017).

Acknowledgements

The project was supported by the Scientific and Technological Research Council of Turkey (TÜBİTAK) with 2210-C Domestic Priority Areas Master's Scholarship and by Erciyes University Scientific Research Projects Office with the project code FYL-2022-11694.

Author contributions

N. T. run all experiments as a first author. I.A synthesized and characterized DHLA-Ala, S.D., M.N. and N.U. contributed to experiments. I.O. conceived the original idea and designed the project. N.T., S.D., and N.U., I.A. and I.O. mainly wrote the manuscript.

Declarations

Competing interests
The authors declare no competing interests.

Additional information
Supplementary Information The online version contains supplementary material available at https://doi.org/10.1038/s41598-024-76772-5.

Correspondence and requests for materials should be addressed to I.O.

Reprints and permissions information is available at www.nature.com/reprints.

Publisher's note Springer Nature remains neutral with regard to jurisdictional claims in published maps and institutional affiliations.